PAPER • OPEN ACCESS

Experimental Device for the Determination of Fracture Toughness at High Pressure

To cite this article: A Muñoz-Ibáñez *et al* 2023 *IOP Conf. Ser.: Earth Environ. Sci.* **1124** 012024

View the article online for updates and enhancements.

Experimental Device for the Determination of Fracture Toughness at High Pressure

A Muñoz-Ibáñez[1,2], M Herbón-Penabad[1] and J Delgado-Martín[1]

[1] School of Civil Engineering, University of A Coruña, Campus de Elviña s/n, A Coruña, 15071, Spain
[2] CINTECX, University of Vigo, GESSMin Group, Department of Natural Resources and Environmental Engineering, Vigo, Spain

jorge.delgado@udc.es

Abstract. Mode I fracture toughness (K_{IC}) is a relevant property in many applications involving rock mechanics. However, the conventional methods for its determination only consider ambient pressure conditions. Although the available experimentation on high pressure fracture toughness shows that K_{IC} tends to increase with confining pressure not all the published results provide with the same evidence. Among the available methodologies for K_{IC} testing, the pseudo-compact tension (pCT) test approach provides with a number of operational advantages over other alternatives and makes it a good candidate for its extension to high pressure research. Based on it, we have designed and constructed a simple high-pressure cell that may be easily installed in any conventional compression frame without modifications to test pCT specimens. The cell may accommodate either a gas or liquid as confining fluids and work with samples of up to 50 mm (~2") diameter. In order to verify the expected performance, we have conducted different calibration tests, including leak rate and the assessment of axial friction. For the demonstration and validation of the experimental approach presented, we have selected virtually impervious poly-methacrylate (PMMA) and Corvio sandstone samples. Results obtained at room conditions and at high pressure are compared and discussed.

1. Introduction

Mode I fracture toughness (K_{IC}) quantifies the capability of a material to resist the tensile stresses conducting to the growth of pre-existing cracks or flaws [1]. Considering that rocks and related materials (i.e. geomaterials) contain discontinuities such as pores, grain boundaries, or foliation, fracture toughness may have paramount importance in rock engineering projects [2-4]. Worth mentioning among them are those involving thermal (geothermics, high-level radioactive waste disposal, etc.), mechanical (pillar/cave stability in mining, etc.) or hydraulic/chemical (hydraulic stimulation, geological storage of CO_2, underground coal gasification, etc.) phenomena as well as in process (drilling and cutting, ore crushing, etc.) and materials (concrete, ceramics, asphalts, etc.) engineering.

Based on fracture mechanics premises, K_{IC} must be an intrinsic material property. Accordingly, its experimental determination should render consistent results irrespective of factors such as the geometry of the specimen or the testing method. However, when applied to rocks, the experimental evidence demonstrates that the K_{IC} values reported in a number of studies contend with such generally assumed behavior. Indeed, significant discrepancies on K_{IC} values can be identified from publications using the same rock type but different testing methods [5-8]. In addition, and as previously reported by different authors, factors such as moisture content, temperature, confining pressure, or pore pressure, are expected

to affect fracture toughness [9,10]. Although the conventional testing methods have been designed to be performed under ambient conditions, this approach may not be sufficient for the determination of fracture toughness in rock, for which stresses always play a significant role in failure mechanisms.

Although studies are still scarce, in recent years significant efforts have been made to adapt fracture toughness testing methods to be conducted under high pressure conditions [11-14]. Results suggest that there is a general increase in fracture toughness with increasing confining pressure due to a reduction of the effective length of pre-existing flaws and cracks [15]. However, not all the published results provide with the same evidence, and some authors have recently argued that this may be related with the lack of standardized procedures. The limited number of experimental works available illustrate that there is still a gap in data and knowledge of K_{IC} measurement in the lab under field realistic conditions.

To contribute to the improvement of the experimental assessment of mode I fracture toughness at high pressure conditions, in this work we present a simple high-pressure cell to perform pseudo-compact tension (pCT) tests at a maximum pressure of 15 MPa. Among the available methodologies for K_{IC} testing, the pCT test approach provides with a number of operational advantages over other alternatives (reduced sample size, precise control of crack propagation, pure tensile loading, simple preparation, etc.) and makes it a good candidate for its extension to high pressure research [16]. This study is focused on the verification of the performance of the testing device and the validation of the experimental approach. To accomplish that, we have conducted different calibration tests including the leak-off rate of the cell and the assessment of axial friction. In addition, we have assessed K_{IC} at ambient and high-pressure conditions using two reference materials, polymethyl-methacrylate (PMMA) and Corvio sandstone.

2. Methodology

2.1. Materials and sample preparation
As previously mentioned, PMMA and Corvio sandstone samples were used in this study. PMMA (also known with the trade-names of Perspex®, Plexiglass® or Lucite®) is a transparent brittle-elastic polymer of high strength and rigidity. Reference values for the compressive strength (σ_c = 83-124 MPa), tensile strength (σ_t = 30-76 MPa) or elastic modulus (E = 2950-3300 MPa) of this material at room temperature are reported in the literature [17,18]. In this work, PMMA specimens for pCT tests were obtained from 50-mm diameter bars, that were sliced into discs (thickness-to-diameter ratio of ~0.5) using a lathe. Then a U-shape groove was carved in the discs to allow sample loading, and a straight notch was also cut to act as stress concentrator (figure 1a).
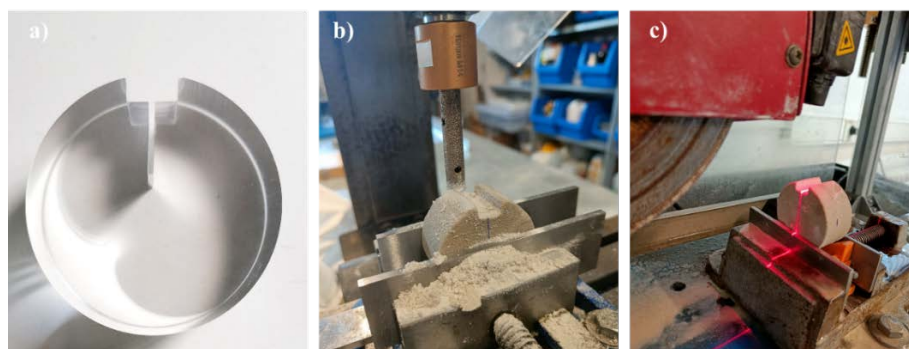

Figure 1. a) PMMA sample; b) Cutting the groove in a sandstone sample using a milling machine; b) Cutting the notch in a sandstone sample with a saw disc.

Corvio sandstone is a grain-supported quartzarenite with microcrystalline silica cement, and it has a relatively low strength (σ_c = 35.4-44.4 MPa; σ_t = 1.9-3.1 MPa), high porosity (18.4-23.5 %) and low elastic modulus (E = 9.7-19.7 MPa) [19]. Corvio sandstone samples were obtained from rock cores of 50 mm in diameter. In this case, the groove was cut in the discs using a milling machine while the notch was introduced with a diamond saw disc, as shown in figures 1b and 1c, respectively. In both cases, the

sample was hold in place thanks to the aid of a vise, and water was used as cooling fluid. After preparation, the samples were oven dried at 60º for 24 hours.

Isopar H (Solvech) was selected as confining fluid for the experiments performed at high-pressure. Isopar H is a colorless, odorless isoparaffinic hydrocarbon solvent with a density and viscosity at 25ºC of 0.76 g/cm^3 and 1.35 cP, respectively [20].

2.2. Testing equipment

A pressure cell was specifically designed to perform pCT experiments under confining pressure. The cell, which can accommodate fluids as well as gas, has been manufactured in 6082 Al-Zn alloy with the T6 thermal treatment (Young's limit and tensile strength of ~69GPa and ~270 MPa, respectively). The inner space of the device is 12.5 cm in diameter and 12.4 cm in height (figure 2a), allowing to work with samples of 50 mm (~2") in diameter. Following the pCT approach, the tensile load is transmitted to the specimen through a couple of steel jaws that penetrate into the groove cut in the specimen. As seen in figure 2b, the jaw on the top remains static while the jaw on the bottom, which is connected to a vertical piston that penetrates into the lid of the cell, is movable. The jaws were manufactured with a circular shape (figure 2c) to guarantee that the applied load is distributed linearly along the groove, reducing the stress concentration in the contact with the specimen, as reported in [16].
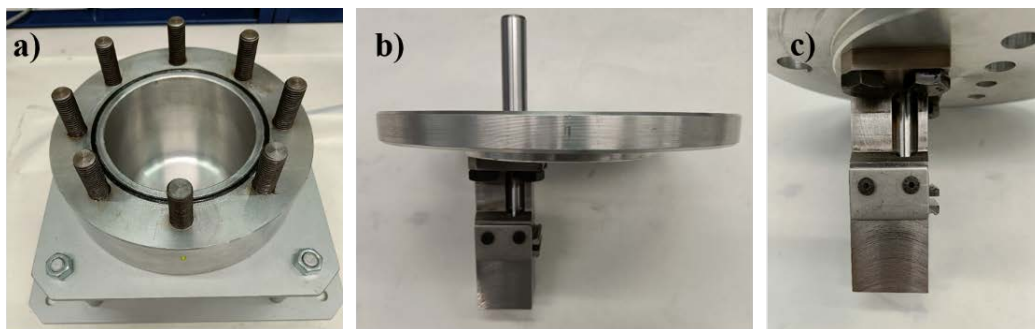

Figure 2. a) Inner view of the cell; b) Top lid of the cell, and piston inserted; c) Detail of the jaws used to deliver the load to the specimen.

The cell may be easily installed in any conventional compression frame without modifications. This is possible thanks to its mechanical configuration that allows to deliver true tension to the notch of the sample while the axial actuator operates in compression over the loading piston. To perform the experiments, the cell was installed in a stiff servo-electric frame equipped with a 50 kN load cell. In this configuration, the displacement of the mobile jaw is given by the movement of the axial actuator of the frame, that inserts the loading piston into the cell. To ensure that the piston is correctly aligned with the axial actuator, the cell is positioned in the frame with the aid of a pin on its base. Feed-throughs on top of the vessel allow to attach up to 8 wires as well as 2 fluid lines for delivering and releasing confining pressure (σ_{conf}). The confining pressure in the cell is monitored using a pressure transducer in the inlet flow line and readings are recorded on a computer. Although not considered in the present study, the sample may be further instrumented with acoustic emission as well as other in-vessel sensors.

2.3. Testing procedure

In order to check the performance of the pressure cell, we have conducted different calibration tests. On one hand, we measured the leak rate by injecting nitrogen gas (N_2) into the cell using the experimental setup shown in figure 3a. The vessel was connected to a pressurized bottle of N_2 and injection pressure (P_{inj}) was controlled until reaching the targeted value (5, 7.5 and 10 MPa). Leak-off rate was monitored using the pressure transducer mounted on the inlet flow line.

On the other hand, we also assessed the axial friction of the loading piston at ambient (0.1 MPa) and high-pressure (5, 10 and 15 MPa) conditions. To this end, the cell was filled with the confining fluid

and pressurized with the aid of a high-pressure pump (Teledyne ISCO 100DX) used for fluid injection (figure 4b). Then the axial actuator of the compression frame (figure 4c) was moved up to a distance of 2 mm at a displacement rate of 0.1 mm/min, following the testing procedure described in [20]. During the tests, we recorded the load delivered by the axial actuator until a constant value was reached (P_{fric}). In addition, we also assessed P_{fric} at ambient pressure without confining fluid, to allow comparison with the experimental results previously reported for the original pCT testing device.

Figure 3. a) Experimental setup for measuring leak-off rate; b) Experimental setup for fracture toughness testing and ISCO pumps; b) Pressure cell placed in the hydraulic press and detail of the flow lines for applying (inlet; right) and releasing (outlet; left) confining pressure.

Finally, we analyzed the performance of the testing approach at ambient (with and without confining fluid) and high-pressure (up to 12.5 MPa) conditions using the two reference materials described in section 2.1. To perform the tests at ambient conditions, samples were attached to the jaws with the aid of a rubber band, as shown in figure 4a. Afterwards, they were fastened inside the pressure vessel and loaded at a constant displacement rate (0.1 mm/min) with both fluid lines open to ambient pressure. In the case of the experiments at high-pressure, the cell was connected to the injection pump and confining pressure was applied before loading the sample. Load (P) and load point displacement (LPD) were recorded continuously during testing. LPD corresponds to the vertical displacement of the mobile (lower) steel jaw, delivered by the axial actuator of the frame.

2.4. Calculations

Level I testing was considered in this study and, therefore, only the value of maximum load (P_{max}) recorded was considered to compute mode I fracture toughness of PMMA and Corvio sandstone. K_{IC} was calculated using the expression given in [16] for the pCT specimen:

$$K_{IC} = Y' \frac{(P_{max} - P_{fric})}{bB} \sqrt{\pi a} \qquad (1)$$

where a is the notch length, b is the distance from the base of the groove to the bottom of the specimen, P_{fric} is the frictional force of the axial actuator, and Y' is the dimensionless stress intensity factor given by the following equation:

$$Y' = C_0 + C_1\left(\frac{a}{b}\right) + C_2\left(\frac{a}{b}\right)^2 + C_3\left(\frac{a}{b}\right)^3 + C_4\left(\frac{a}{b}\right)^4 \quad (2)$$

Coefficients C_o to C_4 are listed in [16]. The effect of the confining pressure was not considered in the previous equation: as the notch remained uncovered during testing (i.e., the confining fluid could penetrate into this region), hydrostatic conditions were achieved and the stress distribution could be assimilated to that computed at ambient conditions [21].
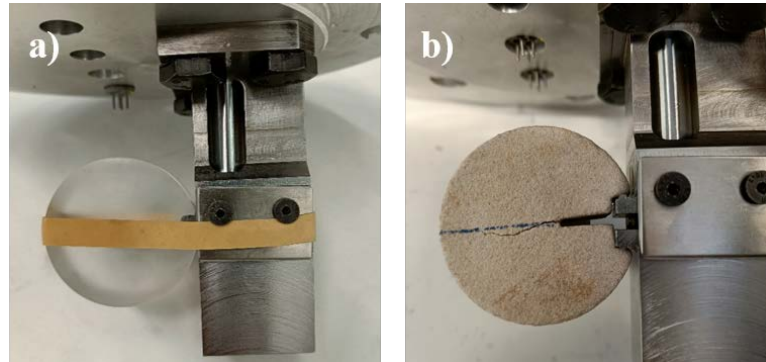

Figure 4. a) PMMA sample before testing; b) Corvio sandstone sample after testing.

3. Results and discussion

Results of the leak-off test using nitrogen gas as confining fluid are plotted in figure 5a. As seen in the graph, although the leak rate is almost negligible at a confining pressure of 5 MPa (< 0.001 MPa/min), it increases at 7.5 MPa (~0.01 MPa/min) and specially at 10 MPa (~0.05 MPa/min). However, it is important to note that the leak flow depends on the properties of the fluid (i.e., the higher the viscosity, the less it leaks [22]), so that a leak test performed with N_2 will be much more sensitive than with the confining fluid selected (Isopar H). Therefore, the leak-off rate recorded is acceptable taking into account the short duration of the tests and the fact that pressure is kept constant by the pump system.
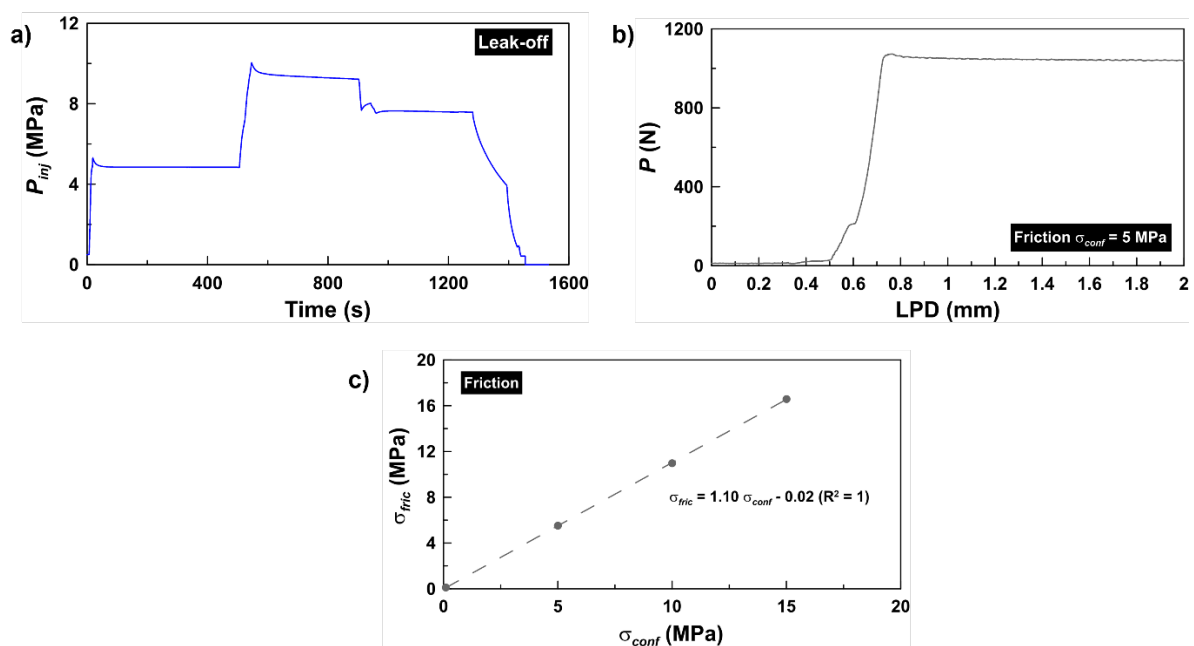

Figure 5. a) Time evolution of injection pressure (P_{inj}); b) P-LPD curve due to axial friction at 5 MPa of confining pressure; c) Friction stress (σ_{fric}) vs confining pressure (σ_{conf}).

Figure 5b shows the results of one of the calibration tests (at 5 MPa of confining pressure) used to assess the axial friction of the piston. The load shows a linear rise up to a maximum value of 1073 N. This first stage, which corresponds to the static friction, reflects the force required to initiate motion. Beyond this threshold, there is a period in which the load decreases and then remains almost constant at ~1040 N. This second stage represents the kinetic friction (i.e., the opposition offered by the piston once in motion (P_{fric}) for the given confining pressure). Results from the tests performed with up to a pressure of 15 MPa (figure 5c) denote that there is a linear relationship between the confining pressure (σ_{conf}) and the friction stress ($\sigma_{fric} = P_{fric}/A$, where A is the area of the loading piston). In fact, the magnitude of the slope suggests that the friction of the loading piston inside the lid would be ~10% of the value of confining pressure applied.

Figure 4b shows a recovered Corvio sandstone specimen after testing, in which a fracture propagated from the notch tip along the ligament plane. Typical load vs load point displacement (P-LPD) curves for the two materials tested in this study under different confining pressures are provided in figures 6a (PMMA) and 6b (Corvio sandstone). All the curves show that the load increases up to P_{max} and, beyond this threshold, it decreases abruptly for PMMA (brittle failure) and more steadily for Corvio sandstone (ductile failure). The testing configuration presented here allowed good control on fracture propagation along the whole duration of the experiments, even in the post-peak region, independently of the confining pressure. However, some differences are observed in the slope of the elastic region (i.e., the linear part of the curve in the pre-peak region) of the two materials when tested at different confining pressures. The variations reported for the last material could be related to its chemical incompatibility with the confining fluid [23] that would induce the softening of PMMA. However, this is not the case for Corvio sandstone, since no adverse oil/rock interaction effects should be expected [24].
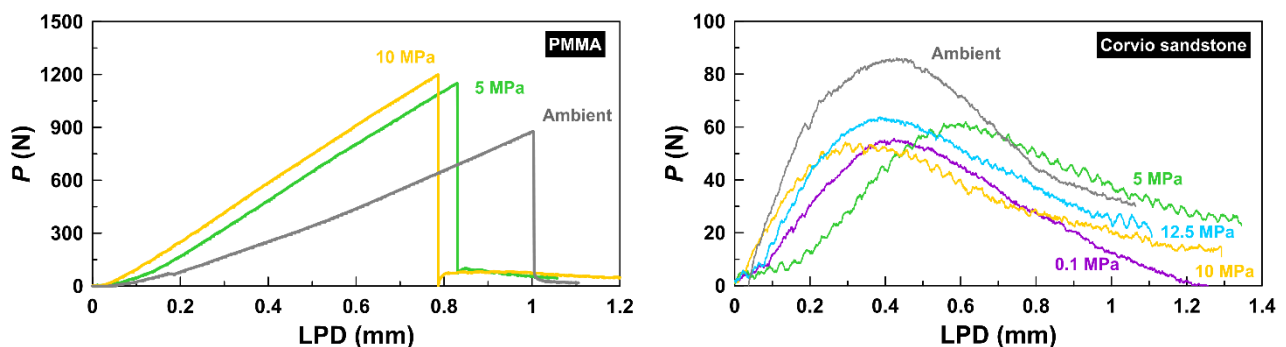

Figure 6. P-LPD curves for PMMA (left) and Corvio sandstone (right).

Regarding fracture toughness results, the value of K_{IC} obtained at ambient conditions and no confining fluid for PMMA was 1.53 MPa m$^{1/2}$ ± 0.02 (n = 2) which is lower than that recorded previously using the conventional pCT approach (1.80 MPa m$^{1/2}$) [25]. Contrary, in the case of the Corvio sandstone, K_{IC} was slightly larger (0.14 ± 0.02 MPa m$^{1/2}$; n = 3) than the range provided in [26] for the same material and specimen size (0.07-0.12 MPa m$^{1/2}$). Values of mode I fracture toughness are plotted as a function of the confining pressure in figure 7. While K_{IC} increases almost linearly with σ_{conf} for PMMA samples, a relationship is not so evident in the case of Corvio sandstone. It would be expected that the resistance of the material will increase under confining stress, as in mode I loading the tensile stress at the crack tip has to overcome the compressive stress induced by the confining pressure [14]. However, it must be noted that the porous sandstone samples tested in this study were not sealed and, therefore, confining fluid could penetrate into the pore space. In this situation, the pore pressure generated inside the sample may have an effect on the strength of the material [27]. This may explain the lower influence of confining pressure on K_{IC} observed for Corvio sandstone, and why the PMMA samples with negligible porosity [30] behaved as expected. However, further testing is needed to confirm this conjecture.
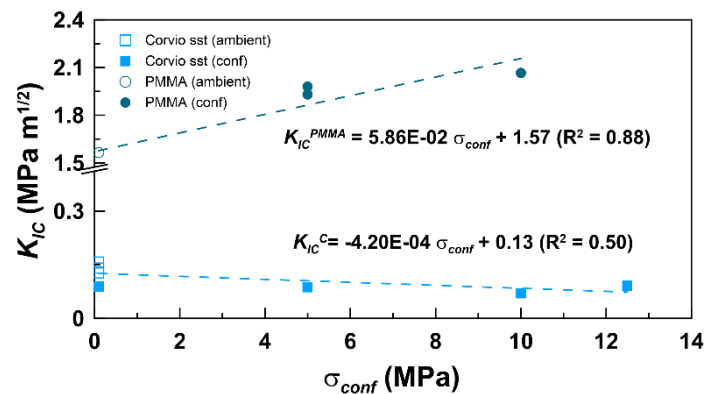
Figure 7. *P*-LPD curves for PMMA (left) and Corvio sandstone (right).

4. Conclusions

In this paper, a high-pressure cell designed to conduct mode I fracture toughness tests under pure tensile conditions was presented and described. The testing approach is based on the experimental concept of the *p*CT test, which has been proven to be convenient for the assessment of K_{IC} in both fragile and ductile rocks. The performance of the pressure vessel was firstly verified by conducting a series of calibration tests. The leak rate measured up to 10 MPa should be admissible when conducting fracture toughness tests using Isopar H as confining medium. Regarding the friction of the loading piston inside the lid, it was estimated at ~10% of the magnitude of confining pressure. Finally, fracture toughness was assessed using two reference materials, PMMA and Corvio sandstone, up to confining stress of 12.5 MPa. Preliminary results suggest that K_{IC} results are comparable to those obtained with the original *p*CT approach at ambient conditions, and that fracture propagation can also be controlled in the post-peak region even at high pressures. Although we report an increase in fracture toughness with confining pressure for PMMA samples, no clear effect was observed for Corvio sandstone, which may be related with the higher porosity of the material.

References

[1]   Whittaker BN, Singh RN and Sun G 1992 *Rock fracture mechanics: principles, design, and applications* (Amsterdam: Elsevier)
[2]   Nasseri MHB, Schubnel A and Young RP 2007 Coupled evolutions of fracture toughness and elastic wave velocities at high crack density in thermally treated Westerly granite *Int J Rock Mech Min Sci* **44** 601-616
[3]   Erarslan N 2016 Microstructural investigation of subcritical crack propagation and Fracture Process Zone (FPZ) by the reduction of rock fracture toughness under cyclic loading *Eng Geol* **208** 181-190
[4]   Talukdar M, Guha Roy D and Singh TN 2018 Correlating mode-I fracture toughness and mechanical properties of heat-treated crystalline rocks *J Rock Mech Geotech Eng* **10** 91-101
[5]   Kataoka M, Yoshioka S, Cho S-H, Soucek K, Vavro L and Obara Y 2015 Estimation of fracture toughness of sandstone by three testing methods *Vietrock2015: An ISRM Specialized Conference. vols. 12–13. Hanoi, Vietnam*
[6]   Erarslan N 2018 The importance of testing method to evaluate the most representative mode I fracture toughness value of brittle rocks *MOJ Civ Eng* **4(5)** 437-441
[7]   Iqbal MJ and Mohanty B 2007 Experimental calibration of ISRM suggested fracture toughness measurement techniques in selected brittle rocks *Rock Mech Rock Eng* **40(5)** 453-475
[8]   Aliha MRM, Mahdavi E and Ayatollahi MR 2017 The influence of specimen type on tensile fracture toughness of rock materials *Pure Appl Geophys* **174(3)** 1237-1253

[9]   Balme MR, Rocchi V, Jones C, Sammonds PR and Boon S 2004 Fracture toughness measurements on igneous rocks using a high-pressure, high-temperature rock fracture mechanics cell *J Volcanol Geotherm Res* **132** 159-172

[10]   Nara Y, Morimoto K and Hiroyoshi N 2012 Influence of relative humidity on fracture toughness of rock: Implications for subcritical crack growth *Int J Solids Struct* **49** 2471-2481

[11]   Kataoka M, Mahdavi E, Funatsu T, Takehara T, Obara Y, Fukui K and Hashiba K 2017 Estimation of mode I fracture toughness of rock by semi-circular bend test under confining pressure condition *Procedia Eng* **191** 886-893

[12]   Stoeckhert F, Brenne S, Molenda M and Alber M 2016 Mode I Fracture Toughness of Rock Under Confining Pressure I*SRM International Symposium - EUROCK 2016, Ürgüp, Turkey*

[13]   Gehne S, Forbes Inskip ND, Benson PM, Meredith PG and Koor N 2020 Fluid-Driven Tensile Fracture and Fracture Toughness in Nash Point Shale at Elevated Pressure *JGR Solid Earth* 125(2) e2019JB018971

[14]   Funatsu T, Kuruppu M and Matsui K 2014 Effects of temperature and confining pressure on mixed-mod (I-II) and mode II fracture toughness of Kimachi sandstone *Int J Rock Mech Min Sci* **67** 1-8

[15]   Yang H, Krause M and Renner J 2021 Determination of Fracture Toughness of Mode I Fractures from Three-Point Bending Tests at Elevated Confining Pressures *Rock Mech Rock Eng* **54** 5295-5317

[16]   Muñoz-Ibáñez A, Delgado-Martín J, Costas M, Rabuñal-Dopico J, Alvarellos-Iglesias J and Canal-Vila J 2020 Mode I fracture toughness determination in rocks using a pseudo-compact tension (*p*CT) test approach *Rock Mech Rock Eng* **53(7)** 3267-85

[17]   Samavedi S, Poindexter LK, Van Dyke M and Goldstein AS 2014 Synthetic biomaterials for regenerative Medicine Applications *Regenerative Medicine Applications in Organ Transplantation* (Academic Press) chapter 7 81-99

[18]   Torabi AR, Saboori B, Keshavarz Mohammadian S, Ayatollahi MR 2018 Brittle failure of PMMA in the presence of blunt V-notches under combined tension-tear loading: Experiments and stress-based theories *Polym Test* **72** 94-109

[19]   Falcon-Suarez I, Canal-Vila J, Delgado-Martin J, North L and Best A 2017 Characterisation and multifaceted anisotropy assessment of Corvio sandstone for geological CO_2 storage studies *Geophys Prospect* **65** 1293–1311

[20]   Farajzadeh R, Andrianov A and Zitha PLJ 2010 Investigation of inmiscible and miscible foam for ehancing oil recovery *Ind Eng Chem Res* **49** 1910-19

[21]   Yang H, Krause M and Renner J 2021 Determination of fracture toughness of mode I fractures from three-point bending tests at elevated confining pressures *Rock Mech Rock Eng* 54 5295-2317

[22]   Strmcnik E and Majdic F 2017 Comparison of leakage level in water and oil hydraulics *Advances in Mechanical Engineering* **9(11)** 1-12

[23]   Industrial Specialties Mfg 2019 Acrylic (PMMA) chemical compatibility chart

[24]   Quick Cut Gasket & Rubber Corporation 2022 Chemical resistance chart

[25]   Muñoz-Ibáez A, Herbón-Penabad M and Delgado-Martín J 2021 Photoelastic stress analysis of mode I fracture toughness tests using PMMA samples *IOP Conference Series: Earth and Environmental Science* **833** 012031

[26]   Muñoz-Ibáñez A, Delgado-Martín J and Juncosa-Rivera R 2021 Size effect and other effects on mode I fracture toughness using two testing methods *Int J Rock Mech Min Sci* **143C** 104785

[27]   Jeffrey RG, Kear J, Kasperczyk D and Zhang X 2015 A 2D experimental method with results for hydraulic fractures crossing discontinuities *49th US Rock Mechanics/Geomechanics Symposium, San Francisco, CA, USA*